Aalborg Universitet

AALBORG UNIVERSITY

DENMARK

Testing Requirements and Control Strategies of Next-Generation Grid Emulator

A Review

Li, Zejie; Ponnaganti, Pavani; Zhao, Fangzhou; Wang, Xiongfei; Bak-Jensen, Birgitte; Munk-Nielsen, Stig; Blaabjerg, Frede

Testing Requirements and Control Strategies of Next-Generation Grid Emulator: A Review

Zejie Li, Pavani Ponnaganti, Fangzhou Zhao, Xiongfei Wang*, Birgitte Bak-Jensen,
Stig Munk-Nielsen and Frede Blaabjerg
Department of Energy, Aalborg University, Aalborg, Denmark
*E-mail: xwa@energy.aau.dk

Abstract—The power-electronic-based grid emulator has been widely used for grid-code compliance testing of wind turbines (WTs). To accommodate the increasing voltage and power levels of WTs, the modular multilevel converter (MMC) emerges as a promising approach for the future grid emulator. This paper provides an overview of testing requirements and control strategies for the MMC-based grid emulator. Specifications, challenges and solutions to implement expected control functionalities of the MMC-based grid emulator are discussed according to testing requirements of WTs. Emerging testing functionalities and future trends of grid emulators conclude this paper.

Keywords— Grid emulator, grid code requirement, testing, modular multilevel converter

I. INTRODUCTION

The power capacity of wind turbines (WTs) has over the years been continuously increasing. The medium-voltage wind turbines with the power capacity of 15 megawatt (MW) will soon be deployed in offshore wind power plants [1]. Consequently, advances in the grid emulation technology are demanded to perform grid-code compliance testing.

There have been several megawatt power-electronic-based grid emulators developed for WTs, notably the 15 MVA grid emulator in LORC, Denmark [2], yet they cannot be used for 15 MW WTs. Recently, a 66 kV/20 MVA grid emulator with a short-circuit power of 80 MVA is being developed for high-power medium-voltage applications [3].

A scalable and versatile grid emulator is demanded to accommodate the increasing power and voltage levels of WTs. The modular multilevel converter (MMC) emerges as a promising approach to meet this demand [4], [5]. The replacement of LC filter by L filter in the MMC enables to widen the bandwidth of voltage control for emulating different grid voltage profiles. In addition to converter topologies, the technical specifications of grid emulators have also been continuously updated, e.g., the injection of 50th harmonic [6] and the overvoltage with 130% of the nominal value [7]. However, it remains unclear whether the technical specifications fulfill the evolution of grid code requirements.

Further, more testing functionalities are furnished with grid emulators, e.g., multi-consecutive faults, stiff/weak grid quantified by grid impedances, and programmable inertial response, etc. Accordingly, the control system of grid emulators is getting more sophisticated with multiple control functions, e.g., impedance control, virtual inertia, fast voltage control, etc. [8]. While these functions can be realized, the grid emulator still differs from actual grids, since its control system can interact with the controller of device under test (DUT), causing unexpected harmonics or even oscillations [2], [8]. Besides the outer interactions, the internal control of MMC, e.g., the submodule voltage balancing, may also interact with external events of grid emulator [9], which further complicates system dynamics and threatens the stability and reliability of grid-code compliance testing.

This paper reviews firstly testing requirements of WTs and identifies technical specifications for next-generation grid emulators. To meet the identified specifications, the required control functionalities of grid emulators are then summarized. The challenges and solutions for realizing control functionalities by the MMC-based grid emulator are elaborated. Finally, two future testing functionalities, i.e., grid-forming capability test and system restoration test are discussed.

II. TESTING REQUIREMENTS AND SPECIFICATIONS OF MMC-BASED GRID EMULATORS

To provide the specifications for the MMC-based grid emulator, the testing requirements of WTs from recently updated grid codes and existing grid emulators are reviewed respect to four aspects, as shown in Fig. 1.

A. Fault-Ride-Through

A crucial testing functionality of grid emulators is the fault-ride-through (FRT) test, i.e., the low-voltage ride-through (LVRT) test and the high-voltage ride-through (HVRT) test. According to IEC 61400-21 [10], IEEE 1547.1 [11] and national grid codes [12]-[16], the testing

Fault-ride-through (FRT)	*Synthetic grid impedance*
• LVRT and HVRT	• Short-circuit ratio (SCR)
Harmonics and power quality	*Frequency response*
• Flicker and THD	• RoCoF & frequency range
• Harmonic interaction	• Inertia

Fig. 1. Testing requirements of WTs.

TABLE I TESTING REQUIREMENTS OF ZVRT, LVRT AND HVRT		
Types	Typical depths of voltage sag/swell	Lasting time of voltage sag/swell
LVRT	0%	<150 ms
	20%	<475 ms
HVRT	130%	<625 ms
	160%	<50 ms

TABLE II FRT REQUIREMENTS OF MULTI-CONSECUTIVE FAULTS		
Fault number	Lasting time of each fault	Fault interval
At least 2 times within 2 min	100 ms	300~500 ms
At least 6 times within 5 min	100 ms	300~500 ms

requirements of FRT specify the typical depths and lasting time of single voltage sag/swell that WTs must withstand, as shown in Table I. Besides, during the fault and the fault recovery, the root-mean-square (RMS) voltage at the point of common coupling (PCC) needs to reach the final value within 20 ms. Moreover, WTs have to remain connected after multi-consecutive symmetrical and asymmetrical faults, as shown in Table II [17].

Additionally, grid codes impose that WTs should be able to regulate reactive current during voltage sags/swell for recovering to the normal operation [17], as shown in Fig. 2. According to the depths of voltage sag and swell, the per-unit (p.u.) value of required reactive current I_q is given by

$$I_{q(p.u.)} = \begin{cases} 0, & \text{if } V_{PCC(p.u.)} \geq 0.9 \\ 2\left[V_{PCC(p.u.)} - 1\right], & \text{if } 0.5 < V_{PCC(p.u.)} < 0.9 \quad (1) \\ -1, & \text{if } 0 < V_{PCC(p.u.)} \leq 0.5 \end{cases}$$

$$I_{q(p.u.)} = \begin{cases} 0, & \text{if } 1 \leq V_{PCC(p.u.)} \leq 1.1 \\ 2\left[V_{PCC(p.u.)} - 1\right], & \text{if } 1.1 < V_{PCC(p.u.)} < 1.5 \quad (2) \\ 1, & \text{if } V_{PCC(p.u.)} \geq 1.5 \end{cases}$$

where the negative I_q represents injection of the reactive current from WTs and the positive I_q denotes absorbing the reactive current from the power grids.

The above FRT test requirements provide the demands for grid emulators in terms of the undervoltage and overvoltage capability, as well as the response time of emulated fault events. Typically, grid emulators using a fast voltage control with 1 kHz~3 kHz bandwidth can emulate 0%~130% of nominal voltage within 20 ms [7], [8]. However, the 130%~160% overvoltage and the multi-consecutive faults are not easy to achieve [7], [18]. Further, the impact of reactive current injection by DUT on the emulated voltage profile is overlooked in existing MMC-based grid emulators [4], [5].

B. Synthetic Grid Impedance

The grid impedance has a significant effect on the grid-code compliance testing of WTs. It is important for grid emulators to have adjustable impedance/admittance for synthesizing various grid impedance values.
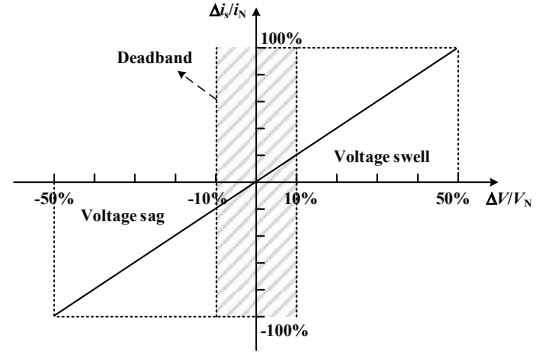

Fig. 2. Requirement of the reactive current output.

The short-circuit ratio (SCR) can be treated as a criterion to evaluate the strength of power grids, which is inverse to the per-unit value of the emulated impedance. An infinite SCR, i.e., ideally stiff grid is realized in a 7 MVA grid emulator [7]. However, the lower limit of emulated SCR remains unclear. The SCR≤1.5 is usually seen as ultra-weak grids and the SCR≥10 is regarded as strong grids. Besides the stiff grid, the grid emulator should synthesize the impedance of actual power grids, i.e., SCR=1.5~10.

C. Harmonics and Power Quality

The power quality is assessed by the voltage flicker test and the measurement of current harmonic emissions of WTs.

The flicker test is used to check voltage fluctuations at the WT terminal during the normal, start and stop of WTs [10]. The reference of flicker generation by the grid emulator is given by

$$u'_{o\_ref} = (1+\delta)u_{o\_ref} \quad (3)$$

where u_{o_ref} is the reference of fundamental frequency output. δ is the low-frequency time-varying signal. The magnitude variation should be within 5% [10].

The current harmonic emissions of WTs should meet grid-code requirements before connecting to power grids. However, the switching operation of converter-based grid emulator may result in additional current harmonics. The IEC 61400-21 standard provides a testing requirement regarding the PCC voltage quality. The total harmonic distortion (THD) of PCC voltage (from 2nd to 50th harmonic) should be below 5% in the no-load operation of grid emulator [10].

Additionally, considering the impact of background harmonics in actual grids on the current harmonics of WTs, the grid emulator is usually required to generate voltage (2nd~50th) harmonics [6]. However, with the high penetration of wide-bandgap power devices, the higher-order background harmonics beyond 50th appear in power grids. Consequently, the higher-order (i.e., 50th~100th) voltage harmonics emulation is to be required for next-generation grid emulators [2], [19].

D. Frequency Response

The purpose of the frequency response test is to check the active power dynamics of WTs under grid frequency variations [10]. The requirements for operating frequency

TABLE III OPERATING FREQUENCY RANGE AND RoCoF

Fundamental frequency (Hz)	Operating frequency range (Hz) (existing/future)		RoCoF (Hz/s)
	min	max	
50 [20]	47/45	52/55	±4
60 [21]	55.5/55	66/66	±4

ranges and the rate of change of frequency (RoCoF) are given in Table III.

According to IEC 61400-21, the grid emulator needs to generate the required RoCoF that is independent on the active power injection of WTs. However, to emulate the actual frequency dynamics, some grid emulators employ the power control to emulate the inertia of synchronous generators (i.e., inertia constant H=2~6 s) [22], which is used to evaluate how the active power of WTs affect the frequency response of power grid.

E. Specifications of Next-Generation Grid Emulators

Recently, with the increase of total capability of wind power, the 66 kV busbar for WTs seems to be a general trend in the wind industry [23]. Moreover, the size of future wind turbines will be in excess of 15 MW, which provides a demand for the next-generation grid emulator with a continuous power rating up to 20 MVA [3].

An oversized design of grid emulators is necessary for the FRT test to withstand a certain short-circuit current from WTs. Generally, an overcurrent capability of 2 p.u. can cover the grid-code compliance test of fully-fed WTs, while the doubly-fed WTs can easily produce 5 p.u. overcurrent during FRT testing [24]. Further, the range of power capability for existing doubly-fed WTs is about 1MW~7 MW and emerging high-power wind platforms are fully-fed WTs. Thus, a 40 MVA short-circuit power is recommended for the future grid emulator.

According to the grid-code requirements and expected functions, technical specifications of future grid emulator are identified in Table IV.

TABLE IV TECHNICAL SPECIFICATIONS OF FUTURE GRID EMULATOR

Terms	Value
Rated line-to-line voltage	66 kV
Rated power	20 MVA
Short-circuit power	40 MVA
Undervoltage capability	0%
Overvoltage capability	160%
Multi-consecutive fault emulation	Yes
Response time of emulated faults	<20 ms
Ideally stiff grid emulation	Yes
Synthetic impedance for actual grids	1.5~10 (SCR)
Max. magnitude of voltage flicker	5%
No-load THD of PCC voltage (2nd~50th)	<5%
Harmonic injection	2nd~100th
Inter-harmonic injection	0.01 Hz~6 kHz
Operating frequency range	45 Hz ~66 Hz
Fast frequency control	±4 Hz/s (RoCof)
Synthetic inertia instant	0~6 s

III. CONTROL FUNCTIONALITIES AND STRATEGIES

To meet the identified specifications, six required control functionalities and corresponding external control of MMC-based grid emulators are shown in Fig. 3. This section presents firstly challenges and solutions of these external control strategies. Further, prospects on the internal control to decouple the interactions of internal and external dynamics are discussed.

A. Voltage Control

The dual-loop voltage control [25]-[27] and the single-loop voltage control [28] are usually adopted with grid emulators, which can also be applied to the MMC-based grid emulator, as shown in Fig. 4. The voltage controller (VC) is employed to realize accurate voltage regulation at the point of common coupling (PCC). Generally, the current controller (CC) of dual-loop voltage control utilizes the proportional-integral (PI) or proportional-resonant (PR) controller to guarantee fast overcurrent limitation. In contrast, the proportional (P) controller based active damping (AD) of single-loop voltage control can improve the disturbance injection and prevent a certain overcurrent.

Currently, WTs usually utilize grid-following inverters based on the current control and power control to interface with power grids [29]. Regardless of the dual-loop or single-loop voltage control in the grid emulator,
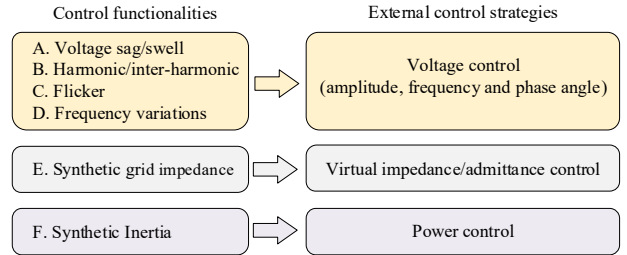

Fig. 3. Control functionalities and external control strategies.
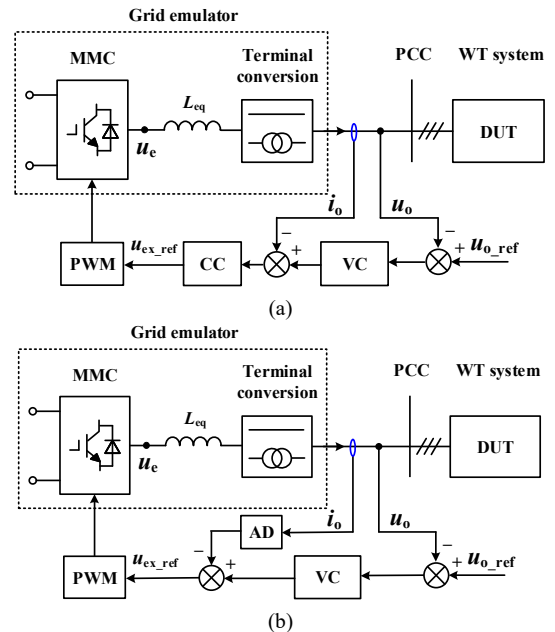

Fig. 4. General diagram for MMC-based grid emulator with DUT. (a) Dual-loop voltage control. (b) Single-loop voltage control.
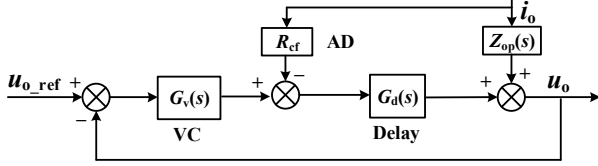
Fig. 5. Single-loop voltage control scheme.

Fig. 6. Outer and inner virtual impedance control.

differing from actual grids, the unexpected current control interactions between grid emulator and DUT may deteriorate system robustness or even introduce harmonic instabilities [30].

To mitigate the adverse current control interactions between grid emulator and DUT, the passivity-based design method of voltage control for the grid emulator is an essential solution. For example, similar to the voltage source inverter (VSI) with LC filter, a wide medium-frequency non-passivity region appears in the single-loop voltage-controlled MMC system [31]. The AD with passivity-based design is usually used to mitigate the above non-passivity [31], [32], as shown in Fig. 5. When the VC adopt the resonant controller, the output impedance and the sign of real part of output impedance can be expressed as

$$Z_o(s) = \frac{(s^2 + \omega_1^2)(sL_{eq} + R_{cf}e^{-sT_d})}{s^2 + \omega_1^2 + sK_{r1}e^{-sT_d}} \quad (4)$$

$$\text{sgn}\{\text{Re}\{Z_o(j\omega)\}\} = \text{sgn}\left\{\left(R_{cf} + \frac{\omega^2 L_{eq}K_{r1}}{\omega_1^2 - \omega^2}\right)\cos(\omega T_d)\right\} \quad (5)$$

where L_{eq} denotes the equivalent inductance. K_{r1} and ω_1 are the resonant gain and fundamental angular frequency. T_d is time delay and R_{cf} is the AD.

To guarantee the passivity of output impedance within the critical frequency $1/(4T_d)$, R_{cf} should satisfy

$$R_{cf} \geq \frac{(\pi/(2T_d))^2 L_{eq}K_{r1}}{(\pi/(2T_d))^2 - \omega_1^2} \approx L_{eq}K_{r1} \quad (6)$$

B. Synthesis of Grid Impedance

The series RL impedance is commonly synthesized by grid emulators [33]. The inner and outer virtual impedance (VI) control are typical impedance-emulation schemes, as shown in Fig. 6, where $Z_v(s)=R_v+sL_v$, R_v and L_v are virtual resistance and inductance respectively [34].

It is essential to first discuss which scheme can represent grid strength through accurate grid impedance emulation. The output impedance of inner and outer VI control is given by

$$\begin{cases} Z_{GE\_outer}(s) = \dfrac{1}{1+T(s)}Z_{op}(s) + \dfrac{T(s)}{1+T(s)}Z_v(s) \\ Z_{GE\_inner}(s) = \dfrac{1}{1+T(s)}Z_{op}(s) + \dfrac{G_d(s)}{1+T(s)}Z_v(s) \end{cases} \quad (7)$$

where $T(s)=G_v(s)G_d(s)$ is the open-loop gain.

The output impedance at fundamental frequency ω_1 represents grid strength. Besides, the magnitude of open-loop gain $T(j\omega_1)$ is an infinite value to guarantee accuracy of output voltage. According to (7), the output impedance Z_{GE_outer} at the fundamental frequency is around $Z_v(j\omega_1)$, while the Z_{GE_inner} is about zero. Therefore, the outer
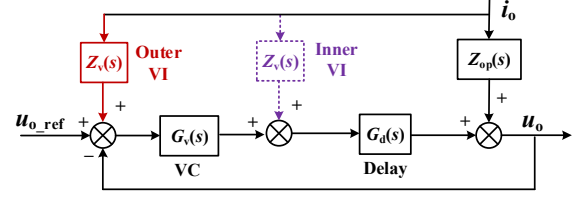
virtual impedance control is better for grid strength emulation than inner virtual impedance.

Secondly, the grid emulator should realize the stiff/ weak grid emulation with transient control functionalities, e.g., voltage sag/swell and flicker, etc. It is crucial to emulate an accurate-transient impedance, which is highly dependent on the bandwidth of voltage control [35].

Although $Z_v(s)=R_v+sL_v$ can represent the steady-state and transient grid impedance, it introduces the derivative term 's', which will amplify the effect of high-frequency measurement noises and even deteriorates system stability. Several derivative-less control techniques for the outer virtual impedance control have been reported in [34]. Among them, the high-pass filter (HPF) and the algebraic-type virtual impedance controller by replacing the 's' with '$j\omega_1$' are two effective methods, as shown in Fig. 7 (a)-(c). Although the HPF can certainly attenuate noises, a high cutoff frequency needs to be used to obtain accurate transient virtual impedance, which worsens the output voltage distortion [36]. Besides the HPF, the algebraic-type controller shows two expressions, i.e., the algebraic approximation and the cross-coupling feedback of current vector. However, they only take effect at the fundamental frequency, which cannot realize accurate impedance emulation with some transient scenarios, e.g., flicker and frequency variations, etc.
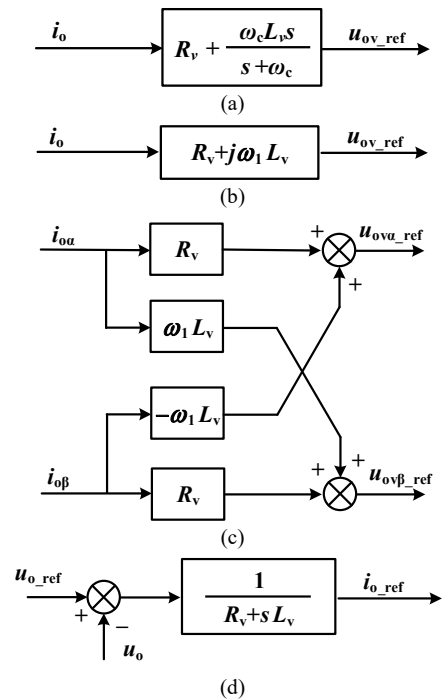

Fig. 7. Feasible controllers for synthesis of grid impedance. (a) HPF. (b) Algebraic approximation. (c) Cross-coupling feedback of current vector. (d) Virtual admittance control.
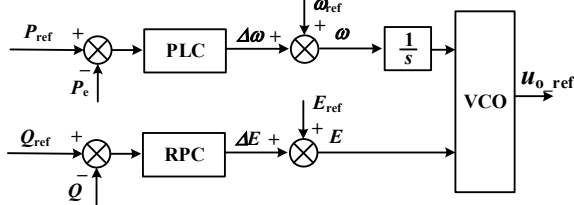
Fig. 8. The power control diagram of grid-forming grid emulator.

Compared to the VI control, the virtual admittance (VA) control is a first-order inertia link $Y_v(s)=1/(R_v+sL_v)$, which not only avoids the derivation term but also realizes a wide-frequency impedance emulation [37], as shown in Fig. 7(d). However, the precise current control has to be utilized to guarantee the accurate output voltage which introduces the serious current control interactions between the grid emulator and the grid-following DUT.

C. Synthesis of Inertia

To emulate the inertia profile, the grid-forming grid emulator needs to enable the power control [8]. A typical power control diagram of grid emulator is shown in Fig. 8. The power loop control (PLC) is designed to emulate the characteristics of inertia and damping. The reactive power control (RPC) is usually implemented by the PI or P controller to provide the voltage magnitude [37]. Four controllers can be applied for the PLC, such as the swing equation-based controller, droop controller with low-pass filer (LPF), PI controller and lead-lag controller [38].

The feasibility of the grid-forming strategy applied in the MMC grid-connection system has been discussed in recent works [39], [40]. However, there are inevitable power control interactions between the grid emulator and a precise power-controlled grid-following DUT, which may affect the accuracy of emulated inertia or even cause the low-frequency resonance [41].

D. Internal Control of MMC

Decoupling the adverse interactions between internal dynamics and external events is crucial for the MMC-based grid emulator. Numerous works adopt the indirect closed-loop modulation method to mitigate the impact of submodule (SM) capacitor dynamics on the output voltage and current [42], [43]. Compared to the direct modulation method, the closed-loop modulation reference is the sum of external and internal control output command divided by the sum of SM capacitor
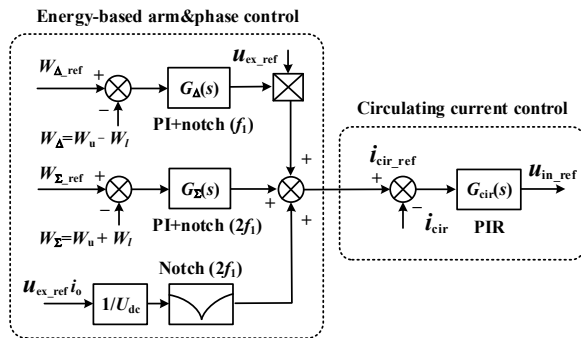

Fig. 9. Energy-based internal control scheme.

voltage instead of the rated DC-link voltage. Therefore, the insertion indices of upper and lower arm can be expressed as

$$n_u = \frac{0.5U_{dc} - u_{in\_ref} - u_{ex\_ref}}{u_{cu}^\Sigma}, n_l = \frac{0.5U_{dc} - u_{in\_ref} + u_{ex\_ref}}{u_{cl}^\Sigma} \quad (8)$$

where n_u and n_l are upper and lower insertion indices. U_{dc} is DC-link voltage. u_{ex_ref} and u_{in_ref} are the external and internal control output reference. u_{cu}^Σ and u_{cl}^Σ are the sum of upper and lower arm capacitor voltage.

According to Fig. 4, the external characteristic equation of MMC-based grid emulator is expressed as

$$L_{eq}\frac{di_o}{dt} = u_e - u_o \quad (9)$$

$$u_e = \frac{n_l u_{cl}^\Sigma - n_u u_{cu}^\Sigma}{2} \quad (10)$$

where u_e is the equivalent output voltage without the equivalent AC inductor L_{eq}.

By substituting (8) into (9) and (10), the characteristic equation of AC side is given by

$$L_{eq}\frac{di_o}{dt} = u_{ex\_ref} - u_o \quad (11)$$

Therefore, the impact of internal SM capacitor dynamics on external output can be mitigated. However, system is unstable without any regulation of SM capacitor voltage [43]. The energy-based arm and phase balancing control and the circulating current control should be employed, as shown in Fig. 9 [44].

The combination of energy-based internal control and grid-forming based external control of MMC is discussed in [45], [46]. It has been demonstrated that by controlling MMC internal energy, the grid-forming based MMC is identical to an equivalent 2-level VSI. Moreover, the feasibility of energy-based internal control used in the MMC-based grid emulator has been validated in [4], [5]. It is shown that steady-state and transient functionalities, i.e., voltage sag and harmonic generation can be emulated by the MMC connected with passive loads.

Although effective, the control dynamics of DUT are neglected. The performance of SM capacitor voltage will be affected by the reactive current injection of DUT. Further, the voltage sag/swell can amplify fluctuations of SM capacitor voltages and circulating current, which may deteriorate system stability and reliability [9]. Therefore, it is essential to mitigate the adverse impact of external-transient events on internal dynamics of the MMC-based grid emulator.

IV. FUTURE TESTING FUNCTIONALITIES

This section evaluates the prospects and challenges of the MMC-based grid emulator for two emerging testing functionalities, which are the grid-forming capability test and the system restoration test.

A. Grid-Forming Capability of DUT

With the development of grid-forming inverters integrated with renewable energy sources, it is essential to test the grid-connection performance of grid-forming DUT, which will promote the evolution of grid code and the structural upgrade of power grids. Partial testing

requirements of grid-forming DUT can be found in [47].

Differing from the grid-following DUT, the grid-forming DUT features the power-based synchronization by the active power control [48]. Besides the outer power control, the inner control of the grid-forming DUT is mainly divided into three categories [49]: 1) single-loop voltage control, 2) dual-loop voltage control, and 3) virtual admittance control with current control, as shown in Fig. 10.

Therefore, the power control interactions between DUT and grid emulator are inevitable if the grid emulator uses the power control for inertia synthesis. Additionally, there have been some voltage control and current control interactions. A reasonable configuration of control strategies in the MMC-based grid emulator can certainly mitigate control interactions between grid emulator and grid-forming DUT, as shown in Fig. 10. Moreover, both MMC-based grid emulator and grid-forming DUT perform as the voltage sources, which presents another challenge for the overcurrent limitation, especially for the transient operating scenarios.

B. System Restoration Capability of DUT

System restoration including black start and re-synchronization is a crucial grid-reconnection capability of DUT after an incidental disconnection caused by the transient faults [2]. It is necessary for the MMC-based grid emulator to test the performance of DUT during system restoration.

In general, a fast re-synchronization process of DUT is often accompanied by a high transient overcurrent [50], which tends to amplify the unbalance of SM capacitor voltage or even threaten system stability. Consequently, more strict requirements are worthy to be provided for the MMC-based grid emulator to mitigate the adverse impact of external events on internal dynamics.
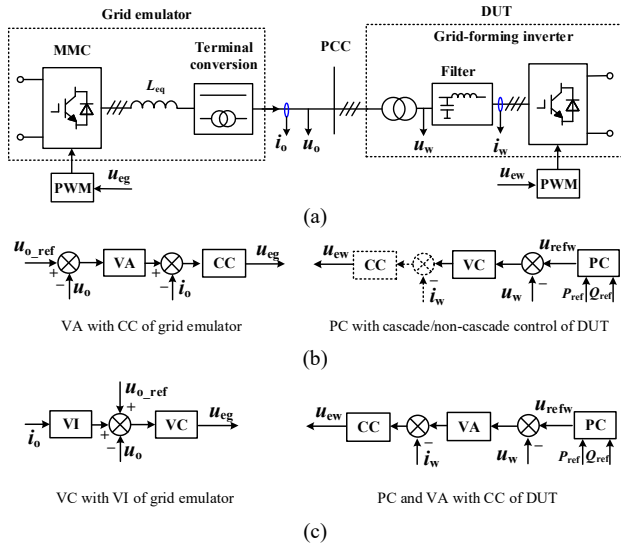

Fig. 10. Configuration of control strategies for the MMC-based grid emulator with grid-forming DUT. (a) General diagram. (b) Control distribution for mitigating the voltage control interactions. (c) Control distribution for mitigating the current control interactions.

V. CONCLUSIONS

This paper has reviewed the testing requirements and control strategies for the MMC-based grid emulator. Based on the requirements of grid codes and the parameters of typical grid emulators, the technical specifications for the next-generation grid emulator are identified. Further, required control functionalities and corresponding external control strategies, i.e., fast voltage control, virtual impedance control and synthetic inertia are summarized. The challenges and feasible solutions are discussed regarding the outer control interactions between grid emulator and DUT, inaccuracy of impedance emulation and inner control interactions of internal and external dynamics.

The more testing functionalities are emerging into the future grid emulator, e.g., grid-forming capability and system restoration capability of DUT. They provide more stricter requirements on mitigating the outer control interactions, limiting the overcurrent and decoupling the interactions between internal control and external transient events.

REFERENCES

[1] IRENA. "Wind energy data," Accessed. Available: https://www.irena. org/wind.

[2] B. Nouri, Ö. Göksu, V. Gevorgian, and P. E. Sørensen, "Generic characterization of electrical test benches for AC- and HVDC-connected wind power plants," *Wind Energy Science*, vol. 5, no. 2, pp. 561-575, 2020.

[3] Fraunhofer. "Fraunhofer IWES launches 20MW simulator," Accessed. Available: https://www.4coffshore.com /news/ fraunhofer-iwes-launches-20-mw-simulator-nid16826.html

[4] M. Jia, S. Cui, K. Hetzenecker, J. Hu, and R. W. De Doncker, "Control of a three-phase four-wire modular multilevel converter as a grid emulator in fault scenarios," in *Proc. ECCE*, Vancouver, BC, Canada, 2021, pp. 624-631.

[5] M. Jia, S. Cui, P. Joebges, and R. W. D. Doncker, "A modular multilevel converter as a grid emulator in balanced and unbalanced scenarios using a delta-wye transformer," in *Proc. ECCE*, Vancouver, BC, Canada, 2021, pp. 2950-2957.

[6] ABB. "ABB's ACS6000 power electronics grid simulator, PEGS, tests medium voltage equipment," Accessed. Available: https://new.abb.com/news/detail/62430/abbs-acs6000-power-electronics-grid-simulator-pegs-tests-medium-voltage-equipment.

[7] P. Koralewicz, V. Gevorgian, R. Wallen, W. van der Merwe and P. Jörg, "Advanced grid simulator for multi-megawatt power converter testing and certification," in *Proc. ECCE*, Milwaukee, WI, USA, 2016, pp. 1-8.

[8] K. Ma, J. Wang, X. Cai and F. Blaabjerg, "AC grid emulations for advanced testing of grid-connected converters-an overview," *IEEE Trans. Power Electron.*, vol. 36, no. 2, pp. 1626-1645, Feb. 2021.

[9] Z. Yin, Y. Yang, and H. Wang, "Transient voltage stress modeling for submodules of modular multilevel converters under grid voltage sags," in *Proc.* ECCE-ASIA, Niigata, Japan, 2018, pp. 1021-1026.

[10] IEC, "Wind energy generation systems - part 21-1: measurement and assessment of power quality characteristics - wind turbines," IEC Std. 61400- 21, 2019.

[11] IEEE, " IEEE standard conformance test procedures for equipment interconnecting distributed energy resources with electric power systems and associated interfaces," IEEE Std 1547.1, 2020.

[12] Technical Regulations TF 3.2.6, "Wind turbines connected to grids with volt- ages below 100 kV," 2004.

[13] "The Grid Code, Revision 47," National Grid ESO, 2020.

[14] "Driftsäkerhetsteknisk utformning av produktion sanläggni ngar," Accessed. Available: https://lagen.nu/svkfs/2005:2.

[15] "Transmission provider technical requirements for the connection of power plants to the Hydro-Quebec transmission system," Hydro Quebec Transenergie, 2009.

[16] H. T. Mokui, M. A. S. Masoum, and M. Mohseni, "Review on australian grid codes for wind power integration in comparison with international standards," in *Proc. AUPEC*, Perth, WA, Australia, 2014, pp. 1-6.

[17] M. Tsili and S. Papathanassiou, "A review of grid code technical requirements for wind farms," *IET Renew. Power Gener.*, vol. 3, no. 3, pp. 308, 2009.

[18] U. Jassmann *et al.*, "Certbench: conclusions from the comparison of certification results derived on system test benches and in the field," *Forschung im Ingenieurwesen*, vol. 85, no. 2, pp. 353-371, 2021.

[19] Wim van Der Merwe, et al. "ABB grid simulator mapping the future, "In *Proc. Annual International Workshop on Grid Simulator Testing of Energy Systems and WT Powertrains*, Golden, Colorado., April 25–26, 2017.

[20] "Nordic Grid Code," ENTSO-E, 2007.

[21] "Interconnection of wind energy," FERC, 2005.

[22] IEEE, " IEEE guide for planning DC links terminating at AC locations having low short-circuit capacities," IEEE Std 1204-1997, 1997.

[23] S. Energy. "Siemens energy to supply transformers for china's first 66 kv offshore wind farm," Accessed. Available: https://press.siemens-energy.com/global/en/pressrelease/siemens-energy-supply-transformers-chinas-first-66-kv-offshore-wind-farm.

[24] J. Morren and S. W. H. de Haan, "Short-circuit current of wind turbines with doubly fed induction generator," *IEEE Trans. Energy Conver.*, vol. 22, no. 1, pp. 174-180, Mar. 2007.

[25] N. R. Averous, M. Stieneker and R. W. De Doncker, "Grid emulator requirements for a multi-megawatt wind turbine test-bench," in *Proc. IEEE Int. Conf. Power Electron. Drive Sys.*, Sydney, NSW, Australia, 2015, pp. 419-426.

[26] A. S. Vijay, S. Doolla and M. C. Chandorkar, "A single back-to-back converter based system emulator for testing unbalanced microgrids," *IEEE Trans. Energy Convers.*, vol. 36, no. 1, pp. 513-523, Mar. 2021.

[27] Y. Hu, J. Cheng, Y. Zhou and G. Chen, "Control strategy of a high power grid simulator for the test of renewable energy grid converter," in *Proc. IEEE IECON*, Beijing, China, 2017, pp. 7747-7752.

[28] S. A. Richter, J. von Bloh, C. P. Dick, D. Hirschmann and R. W. De Doncker, "Control of a medium-voltage test generator," in *Proc. IEEE Power Electron. Special. Conf.*, Rhodes, Greece, 2008, pp. 3787-3793.

[29] M. G. Taul, X. Wang, P. Davari and F. Blaabjerg, "Grid synchronization of wind turbines during severe symmetrical faults with phase jumps," in *Proc. ECCE*, Portland, OR, USA, 2018, pp. 38-45.

[30] X. Wang and F. Blaabjerg, "Harmonic stability in power electronic-based power systems: concept, modeling, and analysis," *IEEE Trans. Smart Grid,* vol. 10, no. 3, pp. 2858-2870, May 2019.

[31] Z. Li, Y. Li, P. Wang, H. Zhu, C. Liu and F. Gao, "Single-Loop Digital Control of High-Power 400-Hz Ground Power Unit for Airplanes," *IEEE Trans. Ind. Electron.*, vol. 57, no. 2, pp. 532-543, Feb. 2010.

[32] Y. Liao, X. Wang, and F. Blaabjerg, "Passivity-based analysis and design of linear voltage controllers for voltage-source converters," *IEEE Open J. Ind. Electron. Soc.*, vol. 1, pp. 114-126, 2020.

[33] H. Yu, M. A. Awal, H. Tu, Y. Du, S. Lukic and I. Husain, "Passivity-oriented discrete-time voltage controller design for grid-forming inverters," in *Proc. ECCE*, 2019, pp. 469-475.

[34] X. Wang, Y. W. Li, F. Blaabjerg and P. C. Loh, "Virtual-impedance-based control for voltage-source and current-source converters," *IEEE Trans. Power Electron.*, vol. 30, no. 12, pp. 7019-7037, Dec. 2015.

[35] S. Li, W. Qi, S. Tan, S. Y. Hui and C. K. Tse, "A General approach to programmable and reconfigurable emulation of power impedances," *IEEE Trans. Power Electron.*, vol. 33, no. 1, pp. 259-271, Jan. 2018.

[36] P. Rodriguez, I. Candela, C. Citro, J. Rocabert, and A. Luna, "Control of grid-connected power converters based on a virtual admittance control loop," in *Proc. EPE*, Lille, France, 2013, pp. 1-10.

[37] M. G. Taul, X. Wang, P. Davari, and F. Blaabjerg, "Current limiting control with enhanced dynamics of grid-forming converters during fault conditions," *IEEE Trans. Emerg. Sel. Topics Power Electron.*, vol. 8, no. 2, pp. 1062-1073, Jul. 2020.

[38] W. Zhang, A. Tarraso, J. Rocabert, A. Luna, J. I. Candela and P. Rodriguez, "Frequency support properties of the synchronous power control for grid-connected converters," *IEEE Trans. Ind. Appl.*, vol. 55, no. 5, pp. 5178-5189, Sept.-Oct. 2019.

[39] S. Yang, J. Fang, Y. Tang, H. Qiu, C. Dong and P. Wang, "Modular multilevel converter synthetic inertia-based frequency support for medium-voltage microgrids," *IEEE Trans. Ind. Electron.*, vol. 66, no. 11, pp. 8992-9002, Nov. 2019.

[40] J. Zhu, C. D. Booth, G. P. Adam, A. J. Roscoe and C. G. Bright, "Inertia emulation control strategy for VSC-HVDC transmission systems," *IEEE Trans. Power Syst.*, vol. 28, no. 2, pp. 1277-1287, May 2013.

[41] F. Zhao *et al.*, "Control interaction modeling and analysis of grid-forming battery energy storage system for offshore wind power plant," *IEEE Trans. Power Syst.*, vol. 37, no. 1, pp. 497-507, Jan. 2022.

[42] A. Antonopoulos, L. Angquist, and H. P. Nee, "On dynamics and voltage control of the modular multilevel converter,", in *Proc. European Conf. Power Electron. Applic.*, Barcelona, Spain, 2009, pp. 1-10.

[43] L. Harnefors, A. Antonopoulos, S. Norrga, L. Angquist, and H. Nee, "Dynamic analysis of modular multilevel converters," *IEEE Trans. Ind. Electron.*, vol. 60, no. 7, pp. 2526-2537, Jul. 2013.

[44] S. Cui, S. Kim, J. -J. Jung and S. -K. Sul, "A comprehensive cell capacitor energy control strategy of a modular multilevel converter (MMC) without a stiff DC bus voltage source," in *Proc. APEC*, Fort Worth, TX, USA, 2014, pp. 602-609.

[45] E. Sanchez-Sanchez, E. Prieto-Araujo, and O. Gomis-Bellmunt, "The role of the internal energy in MMCs operating in grid-forming mode," *IEEE Trans. Emerg. Sel. Topics Power Electron.*, vol. 8, no. 2, pp. 949-962, Jun. 2020.

[46] E. Rokrok *et al.*, "Impact of grid-forming control on the internal energy of a modular multilevel converter," in *Proc. EPE'20 ECCE Europe*, Lyon, France, 2020, pp. 1-10.

[47] "Model acceptance test guideline," AEMO, 2021.

[48] X. Wang, M. G. Taul, H. Wu, Y. Liao, F. Blaabjerg and L. Harnefors, "Grid-synchronization stability of converter-based resources-an overview," *IEEE Open J. Ind. Appl.*, vol. 1, pp. 115-134, 2020.

[49] R. Rosso, X. Wang, M. Liserre, X. Lu and S. Engelken, "Grid-forming converters: control approaches, grid-synchronization, and future trends - a review," *IEEE Open J. Ind. Appl.*, vol. 2, pp. 93-109, 2021.

[50] M. Amin and Q. Zhong, "Resynchronization of distributed generation based on the universal droop controller for seamless transfer between operation modes," *IEEE Trans. Ind. Electron.*, vol. 67, no. 9, pp. 7574-7582, Sept. 2020.